

Fig. 1. Test setup for specimen 165.2×3.0 -SW-SS-C35.

specimens with steel tube ($D \times t$) sizes of 60.5×2.8 , 76.3×3.0 , 114.3×3.0 , 139.4×3.0 and 165.2×3.0 , respectively. From the curves plotted, it is evident that the strength of each CFASS circular stub column was substantially enhanced by the infilled concrete, indicating that the SWSSC infilled into the CFASS tubes was very effective in strengthening the CFASS tubes.

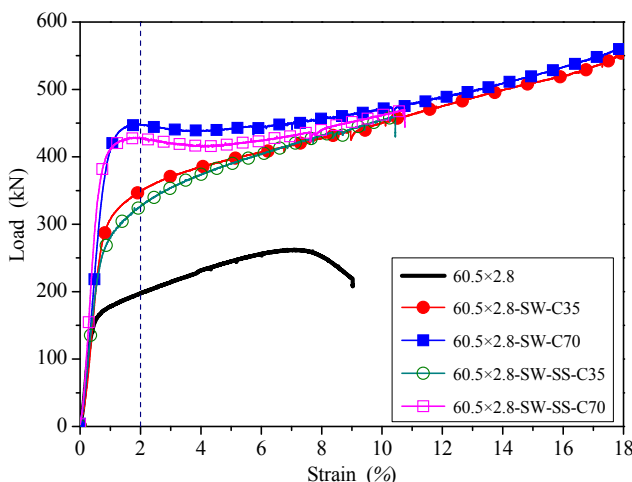


Fig. 2. Load-strain curves of specimens with tube ($D \times t$) size of 60.5×2.8 .

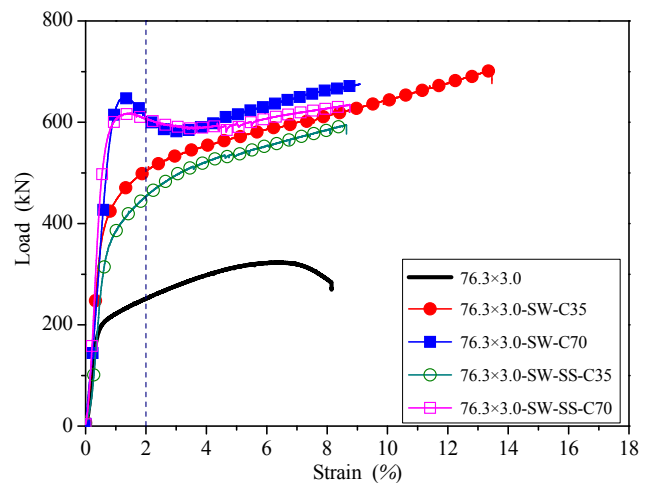


Fig. 3. Load-strain curves of specimens with tube ($D \times t$) size of 76.3×3.0 .

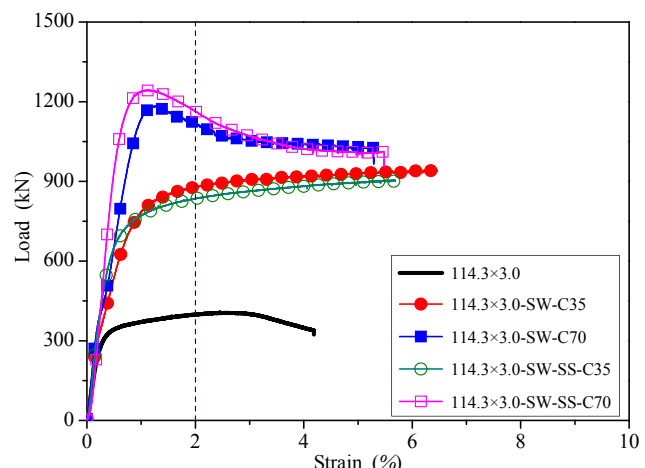


Fig. 4. Load-strain curves of specimens with tube ($D \times t$) size of 114.3×3.0 .

From the load-strain curves, the first peak load within 2% axial strain (P_{peak}), the proof load at 2% axial strain ($P_{2\%}$) and the ultimate load (P_u) are obtained, as tabulated in Tables 5 and 6. It should be noted that sometimes, there was no peak in the load-strain curve within 2% axial strain and the value of P_{peak} in such case is just given as “-”.

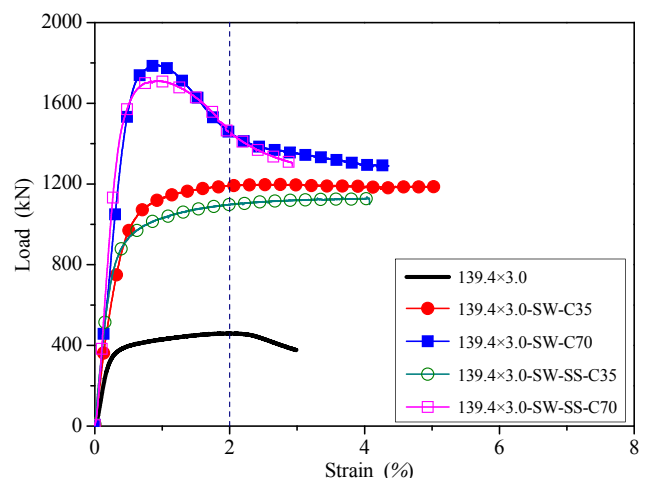


Fig. 5. Load-strain curves of specimens with tube ($D \times t$) size of 139.4×3.0 .



Fig. 8. Failure modes of 60.5×2.8 (left) and $60.5 \times 2.8\text{-SW-C70}$ (right).



Fig. 9. Failure modes of 114.3×3.0 (left) and $114.3 \times 3.0\text{-SW-C70}$ (right).

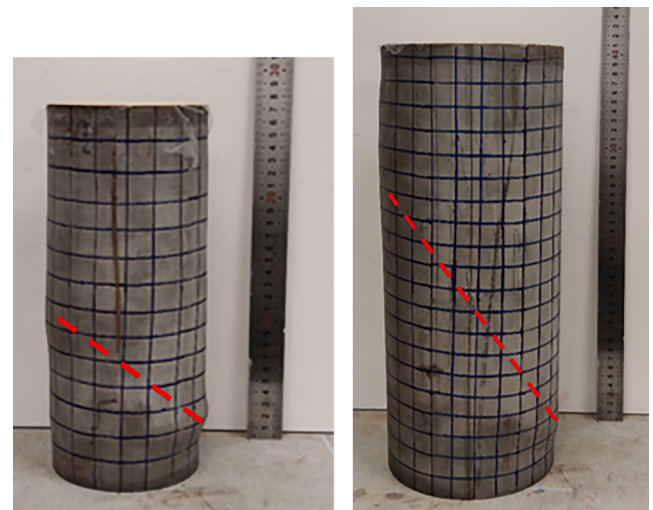


Fig. 11. Failure modes of $114.3 \times 3.0\text{-SW-SS-C70}$ (left) and $165.2 \times 3.0\text{-SW-SS-C70}$ (right).

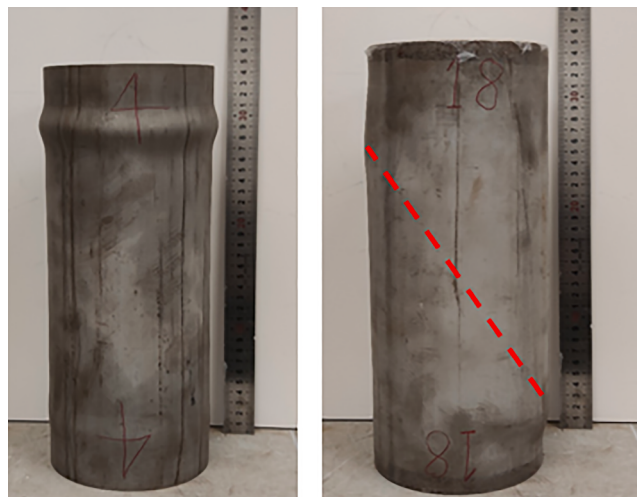
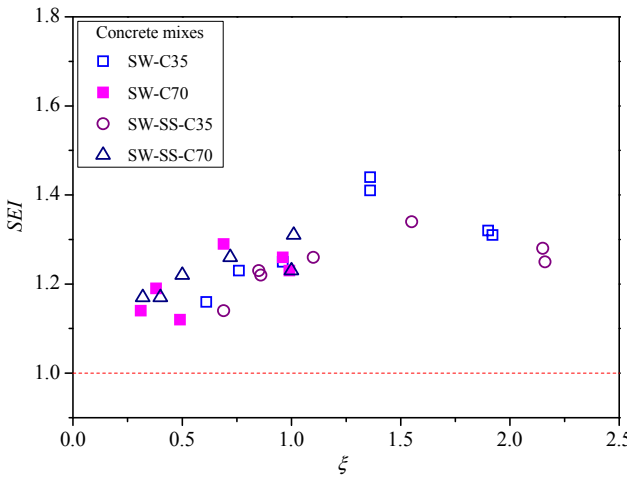
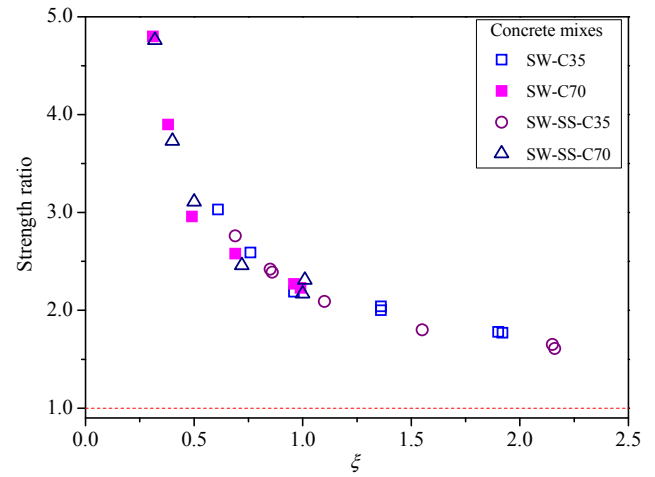
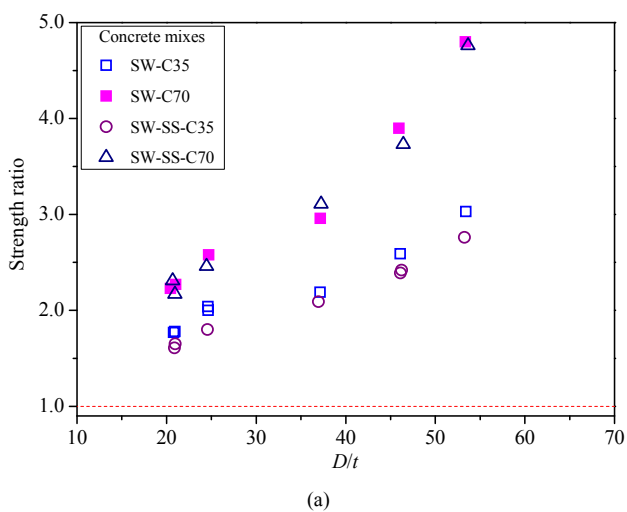


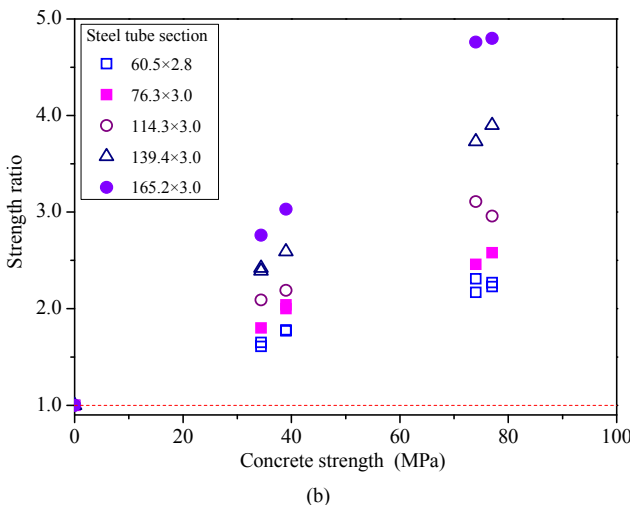
Fig. 10. Failure modes of 139.4×3.0 (left) and $139.4 \times 3.0\text{-SW-C70}$ (right).

strength of the concrete core ($f_c A_c$), where A_s and A_c are the sectional areas of the steel tube and the concrete core, respectively. Such synergistic effects may be quantified in terms of the dimensionless strength enhancement index (SEI) defined by $SEI = P_y/(f_{0.2} A_s + f_c A_c)$. A SEI value of higher than 1.0 indicates positive enhancement of the yield load (P_y) due to the synergistic effects of the composite action. The SEI values of the specimens tested have been calculated, as presented in Table 7. From these SEI values, it can be seen that the SEI varies from 1.12 to 1.44 within range of structural parameters covered in this study.

To analyse how the SEI varied with the various structural parameters, the D/t ratio of the steel tube and the section constraining factor (ξ) defined by $\xi = f_{0.2} A_s / f_c A_c$ are also calculated, as listed in Table 7. Basically, the section constraining factor (ξ) is a measure of how strong the steel tube is relative to the concrete core. Together, the D/t ratio and the section constraining factor (ξ) govern the degree of confinement provided by the steel tube on the concrete core. To visualize the effects of these two parameters, the variation of the SEI with the D/t ratio is plotted in Fig. 13 and the variation of the SEI with the value of ξ is

Fig. 14. Variation of SEI with ξ .Fig. 16. Variation of strength ratio with ξ .

(a)



(b)

Fig. 15. Variations of strength ratio with (a) D/t , and (b) concrete strength.

lowest value of 1.61. This was because a larger D/t ratio and/or a higher concrete strength always lead to a lower ξ value but a higher strength ratio, causing the strength ratio to be inversely related to the ξ value.

4.3. Strain-hardening ductility performance

Whether the specimen had exhibited strain-hardening can be judged from the shape of its load-strain curve. If the load-strain curve, after passing through the point of 2% axial strain, gradually increased to reach an ultimate load (P_u) higher than the yield load (P_y), then it may be said that strain-hardening had occurred. The specimens that had exhibited strain-hardening are marked by "Yes" in the last column of Table 7. Out of the 26 concrete infilled CFASS tube specimens tested, 20 specimens had exhibited strain-hardening and the other 6 had not exhibited strain-hardening. Checking their ξ values, it is noted that those specimens that had exhibited strain-hardening had ξ values of 0.61 or higher, whereas those specimens that had not exhibited strain-hardening had ξ values of 0.50 or lower. Hence, as a rough guide, a minimum ξ value of 0.6 is needed for attaining strain-hardening ductility performance.

5. Assessment of codified design rules

There are still no design rules stipulated in any of the existing codes for the design of stainless steel circular tubes infilled with conventional concrete or SWSSC. Nevertheless, there are some design rules for the design of carbon steel circular tubes infilled with conventional concrete in the Eurocode EC4 [36], Australian Standard AS5100 [37], AISC Specification [38] and ACI Building Code ACI318 [39]. Whether these design rules could be applied also to stainless steel circular tubes infilled with conventional concrete or SWSSC is assessed in the following subsections.

5.1. Eurocode EC4 and Australian Standard AS5100:

The design equations provided in EC4 [36] and AS5100 [37] are the same. In Section 6.7.3 of EC4, the design equation for the nominal strength (P_{EC}) of CFST circular stub column under axial load is given as:

- [33] Li YL, Zhao XL, Singh Raman RK, Yu X. Axial compression tests on seawater and sea sand concrete-filled double-skin stainless steel circular tubes. *Eng Struct* 2018; 176:426–38.
- [34] Dong Z, Wu G, Zhao X-L, Zhu H, Lian J-L. Durability test on the flexural performance of seawater sea-sand concrete beams completely reinforced with FRP bars. *Const Build Mater* 2018;192:671–82.
- [35] Li YL, Zhao XL, Singh Raman RK. Mechanical properties of seawater and sea sand concrete-filled FRP tubes in artificial seawater. *Const Build Mater* 2018;191: 977–93.
- [36] EC4. Eurocode 4: Design of composite steel and concrete structures. 1-1: General rules and rules for buildings control, European Committee for Standardization (CEN) EN 1994-1-1, Brussels, Belgium: CEN, 2004.
- [37] AS5100. Bridge design, part 6: steel and composite construction, AS 5100.6-2004, Standards Australia, Sydney, Australia, 2004.
- [38] AISC. Specification for structural steel buildings, American Institute of Steel Construction, ANSI/AISC 360-16, Chicago, 2016.
- [39] ACI. Building Code Requirements for Structural Concrete (ACI 318M-14) and Commentary (ACI 318RM-14), American Concrete Institute, Detroit, USA, 2014.
- [40] Cai Y, Quach WM, Young B. Experimental and numerical investigation of concrete-filled hot-finished and cold-formed steel elliptical tubular stub columns. *Thin-Walled Struct* 2019;145:106437.
- [41] Uy B, Tao Z, Han LH. Behaviour of short and slender concrete-filled stainless steel tubular columns. *J Constr Steel Res* 2011;67(3):360–78.
- [42] M. Lai. Behaviour of CFST columns with external confinement under uni-axial compression, PhD Thesis (2015), The University of Hong Kong, Hong Kong.
- [43] L. Li. Structural performance of concrete-filled cold-formed stainless steel members, PhD Thesis (2017), The University of Hong Kong, Hong Kong.
- [44] Han L-H, Yao G-H, Zhao X-L. Tests and calculations for hollow structural steel (HSS) stub columns filled with self-consolidating concrete (SCC). *J Constr Steel Res* 2005;61:1241–69.
- [45] Lam D, Gardner L. Structural design of stainless steel concrete filled columns. *J Constr Steel Res* 2008;64(11):1275–82.
- [46] Tam VW, Wang Z-B, Tao Z. Behaviour of recycled aggregate concrete filled stainless steel stub columns. *Mater Struct* 2014;47:293–310.
- [47] Yang Y-F, Ma G-L. Experimental behaviour of recycled aggregate concrete filled stainless steel tube stub columns and beams. *Thin-Walled Struct* 2013;66:62–75.
- [48] M.-G. Lee, Y.-C. Wang, Y.-M. Su, Y.-C. Kan, S.-H. Kao. Effect of cylinder size on the compressive strength of concrete CO₂ curing, In: M. Barman, M. Zaman, J.R. Chang (eds) Transportation and Geotechniques: Materials, Sustainability and Climate. GeoChina 2018. Sustainable Civil Infrastructures, Springer, 2018, pp33–42.